Development of antibacterial steel surfaces through laser texturing

Victor M. Villapún; A. P. Gomez; W. Wei; L. G. Dover; Jonathan R. Thompson; T. Barthels; J. Rodriguez (ID) ;
S. Cox; S. González ✉ (ID)

Check for updates

View Online Export Citation

Development of antibacterial steel surfaces through laser texturing

View Online   Export Citation   CrossMark

Victor M. Villapún,[1,a] A. P. Gomez,[2] W. Wei,[3] L. G. Dover,[4] Jonathan R. Thompson,[4] T. Barthels,[3] J. Rodriguez,[5] (ID) S. Cox,[1] and S. González[6,b] (ID)

AFFILIATIONS

[1] School of Chemical Engineering, University of Birmingham, Edgbaston B15 2TT, United Kingdom

[2] Departamento de Microbiología, Complejo Hospitalario Universitario A Coruña (HUAC),
Instituto de Investigación Biomédica A Coruña (INIBIC), Universidad de A Coruña (UDC), A Coruña, Spain

[3] Fraunhofer-Institut für Lasertechnik ILT, Aachen, Germany

[4] Faculty of Health and Life Sciences, Northumbria University, Newcastle upon Tyne NE1 8ST, United Kingdom

[5] Centro de Investigaciones Científicas Avanzadas (CICA), Departamento de Química, Facultad de Ciencias,
Universidad da Coruna, 15071 A Coruña, Spain

[6] Faculty of Engineering and Environment, Northumbria University, Newcastle upon Tyne NE1 8ST, United Kingdom

[a] Email: v.m.villapun@bham.ac.uk
[b] Author to whom correspondence should be addressed: sergio.sanchez@northumbria.ac.uk

ABSTRACT

The aim of the present study was to develop novel antibacterial touch surfaces through the laser texturing optimization of stainless steel. A wide range of laser fluence (2.11 J/cm^2–5.64 J/cm^2) and scanning interval (10 μm–30 μm) parameters were explored. The impact of surfaces with different patterns, wettability, and oxidation states on the antimicrobial behavior of *Escherichia coli* K-12 and biofilm hyper-producing *Acinetobacter baumannii* MAR002 was assessed. Modification of laser input enacted topographical changes with high scanning intervals leading to ordered surface patterns, while increasing the laser fluence to 5.64 J/cm^2 created larger and less ordered plateaus and valleys. Texturing also drove a transition from a hydrophilic starting surface with a contact angle of 80.67° ± 3.35° to hydrophobic (138°–148°). Antimicrobial analysis and bioluminescence assays of *E. coli*, alongside biofilm forming test through *A. baumannii* MAR002 indicated the ability of laser texturing to produce effective bactericidal touch surfaces. No simple correlation was found between wettability and bacterial behavior, revealing that proliferation is dependent on roughness, oxidation, and wettability. For the conditions selected in this study, a laser fluence of 5.64 J/cm^2 and a scanning interval of 10 μm showcased the lowest amount of recovered bacteria after 30 min.

INTRODUCTION

The number of healthcare acquired infections (HAI) is on the rise, posing a critical socioeconomic hazard. Solely in England, 300 000 patients develop a nosocomial infection annually, while in the United States up to 1.7 × 10^6 incidents take place yearly.[1–3] Antibiotic therapies are the common course of action to tackle HAIs; however, with the emergence of antimicrobial resistance (AMR), patients suffering infections caused by pandrug-resistant pathogens and the number of new drugs in development being reduced, such

an approach may prove difficult in the near future.[4–6] The predictions of AMR socioeconomic impact have shown an estimated cost of $100 trillion, endangering 10 × 10^6 lives annually worldwide by 2050.[7] While this prediction has been labeled uncertain and pessimistic,[8] it is clear to say that AMR is one of the great healthcare challenges of our era. Consequently, there is a critical need to develop and implement novel antimicrobial therapies.

A patient suffering from HAI is a hazard to clinical staff and other patients receiving healthcare treatment, as bacterial species are prone to transmit in these settings. The most common path

responsible for microbial transfer is hand to hand and surface to hand contact between staff, patients, and touch surfaces (e.g., door handles, touch plates, countertops, or switches).[9,10] Cleaning and disinfection can be used to control microbes spreading; nonetheless, special care should be taken with touch surfaces as these are potential reservoirs where micro-organisms can survive from days to even months.[10] To limit the spreading of microbes, a possible solution is to implement antimicrobial surfaces in areas susceptible to bacteria colonization. Numerous antimicrobials are available for such a purpose; however, there has been a prominence to reintroduce old antimicrobial metals (e.g., copper, silver) and photocatalytic elements (e.g., titanium oxides).[11–14] Nevertheless, the cost of copper and silver, coupled with the failure of some photocatalytic surfaces in healthcare settings,[15] has caused a reticence to implement these materials. As such, cleaning protocols are still the most broadly used control approach.[11] That said, topographical modification to prevent bacterial attachment and microbial transfer on touch surfaces, specifically the use of laser texturing, has been gaining interest in the biomaterials community.

Laser texturing is a technique that may be used to modify surface roughness, chemistry, and wettability, all of which have been shown to influence bacterial attachment.[16–18] However, the exact relationship between these properties has not been completely elucidated, and mixed observations can be found in the literature. This is exemplified by surface roughness where values in the nano- to microscale (0.04 μm–3 μm) are reported to generally favor bacterial adhesion as the average roughness is increased.[19,20] Nevertheless, the observations from Shaikh et al.[21] and Taylor et al.[22] support a reduction in the proliferation of some bacterial species as the surface becomes coarser. Such changes in topology can also affect the wettability of the material. As shown by Kubiak et al.,[23] roughness modification can be used to modify the complete wetting mode common to hydrophilic surfaces into a double wetting mode typical of hydrophobic surfaces. From these two wetting modes, generally, hydrophobic (contact angles >90°) materials are considered less prone to bacterial adhesion than hydrophilic (contact angles <90°) surfaces, although the optimal wettability to reduce bacterial adhesion is still controversial.[24,25] Efforts have been made to develop superhydrophobic surfaces that offer anti-adhesive properties with investigations to understand their influence on bacterial adhesion still going on. One such case is textured stainless steel where many authors have previously analyzed its influence on wettability;[26–30] nonetheless, the number of studies focused on the associated antimicrobial behavior is relatively scarce.[31–33] Its low cost and large range of applications makes stainless steel an attractive material to develop antimicrobial touch surfaces. With AMR on the rise and limited new antibiotics on the pipeline, complementary novel strategies to tackle HAIs are required.

The optimization of laser texturing conditions to develop antimicrobial touch surfaces is an area of great potential. In this paper, we systematically assess the effect of laser processing conditions, namely laser fluence and scanning interval, on the physicochemical and antimicrobial properties of textured stainless steel. A bioluminescent *Escherichia coli K*12 strain, a common cause of infections in healthcare, and *Acinetobacter baumannii* MAR002, a high biofilm former, were selected as model micro-organisms, enabling the assessment of the antimicrobial effectiveness in decisive healthcare locations. Moreover, these micro-organisms emulate the colonization of bacteria strains labeled critical by the World Health Organization.[34] This knowledge will be useful for the development of antimicrobial surfaces for hospitals and other healthcare settings.

METHODS

Patterning was performed using laser ablation (Pharos Light Conversion, PHAROS) with a repetition frequency of 200 kHz, a wavelength of 1028 nm, a pulse duration of 200 fs, a spot diameter of 33 μm, and a scanning speed of 20 mm/s. To surface texture the 304 stainless steel samples, two different laser fluences (2.11 J/cm^2 and 5.64 J/cm^2) and scanning intervals (10 μm and 30 μm) were used, resulting in an arrangement of distinctive and well-defined patterns. For simplicity, the textured samples have been coded as F1-30, F1-10, F2-30, and F2-10 according to the laser fluence and scanning interval conditions (Table I).

The microstructure of the base substrate and treated stainless steel was studied by x-ray diffraction (XRD) using a Siemens D5000 diffractometer with Cu Kα radiation (λ = 1.541 84 Å) at 40 kV and 40 mA and a step size of 0.01°/s in the 2θ range 25°–90°. Surface finish was analyzed using an Alicona profilometer (Infinite Focus, Alicona UK, Sevenoaks, United Kingdom) to obtain 3D scans from a 700 × 550 μm^2 area, and the results were obtained averaging ten measurements (ten lines of 600 μm length each perpendicular to the texturing direction). Compositional analysis and surface imaging was performed using a Tescan Mira 3 scanning electron microscope (SEM) with 20 kV of acceleration voltage, equipped with an Oxford Instruments X-Max 150 energy dispersive x-ray (EDX) detector.

Contact angle measurements were carried out using the sessile drop technique (Krüss drop size DSA30 analyzer). A volume of 1 μl of deionized water was dispersed at a rate of 30 μl/min and slowly approached to the sample until contact with the surface was made. Then, an additional 1 μl was dispersed, to ensure the contact angle of the final 2 μl droplet was caused by natural interactions between the liquid and the sample, reducing the effect of syringe movement. Contact angle measurements were performed immediately upon deposition to prevent droplet shape change during evaporation. The contact angle results were averaged from ten sessile drop tests.

Bioluminescence tests were developed using *E. coli* strain K12 transformed with plasmid (pVIB) containing lux genes and cultivated at 28 °C in Luria Bertani (LB) broth with ampicillin. After dilution and re-culturing until OD$_{600}$ ~ 0.3 μl, 2 μl were

TABLE I. Laser processing parameters.

Sample	Laser fluence (J/cm^2)	Scanning speed (mm/s)	Scanning interval (μm)
F1-30	2.11	20	30
F1-10	2.11	20	10
F2-30	5.64	20	30
F2-10	5.64	20	10

inoculated on the samples and bioluminescence was measured using Syngene Gbox XT4 with an exposure time of 1 min.

Antimicrobial tests were performed with the same *E. coli* strain used in the bioluminescence tests. After growing overnight (~16 h), the culture yield was quantified with optical density measurements at 600 nm (OD_{600}) and bacteria were then diluted in sterile LB broth to an optical density of 0.01. The diluted cultures were incubated at 28 °C until an OD_{600} ~ 0.3 was reached. Laser textured and control samples (untextured stainless steel) were then immersed in 100% ethanol and subsequently sonicated for 5 min in an ultrasound bath to ensure a clean and disinfected surface. The disinfected samples were left to dry in a sterile petri dish and then moved into a new sterile petri dish containing tissue paper wetted with 1 ml of sterile LB broth to prevent the samples from drying. A quantity of 1 μl of the previously described culture was dispensed directly onto the textured and control surfaces, following incubation at room temperature in the sealed containers. After the designated exposure time, the samples were diluted in 99 μl of Tween 20 0.148 g/l, 2× critical micelle concentration (CMC), and sonicated for 5 min. Finally, the recovered bacterial suspension was subjected to serial decimal dilution and spread onto LB agar plates with the resulting colonies counted after 16 h of incubation at 37 °C. All tests were performed five times, with mean counts and standard deviation reported.

A biofilm hyper-producing *A. baumannii* MAR002 strain[35] was used to study the influence of laser texturing in biofilm formation. One colony of MAR002 strain grown on agar media was inoculated into 5 ml of LB broth and incubated overnight at 37 °C. The overnight culture was diluted 1:100 in LB broth and 100 μl inoculated in a 96 well plate containing the textured samples. The samples were then incubated at 37 °C for 48 h under static conditions. The materials were then rinsed three times with Dulbecco's phosphate-buffered saline (DPBS) to remove any unbound bacteria and transferred into sterile conical tubes containing 5 ml of DPBS. The tubes were vortexed at full speed for 1 min and then placed in an ultrasonic bath and sonicated for 10 min at a low power intensity, to release the attached bacteria from the material. After an additional vortex step, suspensions were serially diluted with DPBS and cultured overnight. The CFUs were counted to determine the number of viable adherent bacteria; each assay included three independent replicates.

A deeper analysis of biofilm formation on the surface of the different materials tested was performed using Scanning Electron Microscopy (SEM). The material samples incubated as mentioned above were washed, dehydrated in ethanol, processed with a critical point drier, and sputter coated as described previously.[35] Biofilms formed on the laser textured surfaces were viewed using a Zeiss Supra Gemini Series 35V SEM.

RESULTS AND DISCUSSION

Figure 1 shows the SEM images of the stainless steel textured surfaces under F1-30, F1-10, F2-30, and F2-10 conditions along with optical profilometry scans and microscopy images. In contrast to the rough surface showcased by the laser treated coupons, the non-textured as-received sample, used as control in all of the performed tests, displays a relatively smooth surface with small scratches, likely caused during the fabrication process (i.e., rolling). This relatively smooth surface is heavily modified under all assessed laser processing parameters resulting in highly oriented topography dominated by grooves similar to those observed in other laser ablated austenitic steels.[36,37]

The surface roughness was assessed by measuring the arithmetic average roughness (R_a) from the profiles obtained through optical profilometry. For a laser fluence of 2.11 J/cm^2, the decrease in the scanning interval from 30 μm to 10 μm did not notably alter R_a with F1-30 and F1-10 revealing similar values, 8.93 ± 0.97 μm and 8.00 ± 2.13 μm, respectively. However, this decrease in the scanning interval did change the repeatability of the pattern with the F1-30 texture showing more highly ordered grooves along the direction of the laser movement compared to F1-10. This surface exhibited more random and coarser features consisting of high plateaus, up to 50 μm, and low pits, down to 30 μm. A similar trend can be observed for samples F2-30 and F2-10 treated with a laser fluence of 5.64 J/cm^2 and corresponding scanning intervals, i.e., 30 μm and 10 μm, respectively. Nonetheless, a more pronounced increase in R_a was observed, rising from 2.22 ± 0.17 μm to 14.62 ± 1.92 μm for the higher laser fluence, which is consistent with the observations of Wu *et al.*[38] These results confirm that the parallel grooves oriented in the laser direction present an ordered structure for high scanning intervals, which is lost when the scanning interval was decreased from 30 μm to 10 μm. In addition to the topographical changes, the right panels of Fig. 1 show the optical images of the textured and control stainless steel samples, which suggest further modifications to the base substrate. They exhibit a rusted appearance probably associated with the high temperatures and the presence of oxygen reached during the laser treatment. To analyze in detail the chemical modification driven by laser patterning, the XRD scans were obtained for the all treated and untreated samples (Fig. 2).

The XRD scan of the as-received 304 stainless steel [Fig. 2(a)] shows three intensity peaks, which can be correlated with the γ phase (austenite) typical of austenitic steels. The relative intensity of the XRD peaks associated with the γ phase at 43.467°, 50.685°, and 74.763° is different from that of the material in powder conditions obtained from the PDF XRD files.[39] According to the PDF, the maximum intensity peak corresponds to (1 1 1), followed by (2 0 0), and finally (2 2 0), while our XRD results show [Fig. 2(a)] that the maximum intensity is detected for (2 2 0), followed by (1 1 1) and (2 0 0). This discrepancy suggests that the as-received plate exhibits preferential orientation along the (2 2 0) plane likely induced during rolling.

Patterning with a fluence of 2.11 J/cm^2 appears to modify the microstructure [Figs. 2(b) and 2(c)] generated upon rolling, suggesting that the melting of the rolled surface has taken place. In addition, a small peak at about 35.26° and 62.46° attributed to Fe_3O_4 is observed, indicating that the molten surface has undergone some slight oxidation, consistent with the surface morphology (Fig. 1) and the work of Ngo and Chun.[40] Additional peaks corresponding to Fe_3O_4 are observed as the laser fluence rises to 5.64 J/cm^2 for both F2-30 and F2-10 conditions [Figs. 2(d) and 2(e)]. These samples display higher intensity peaks for Fe_3O_4, which increase as the laser scanning speed decreases, followed by an intensity decrease of the diffraction peaks associated with the γ phase.
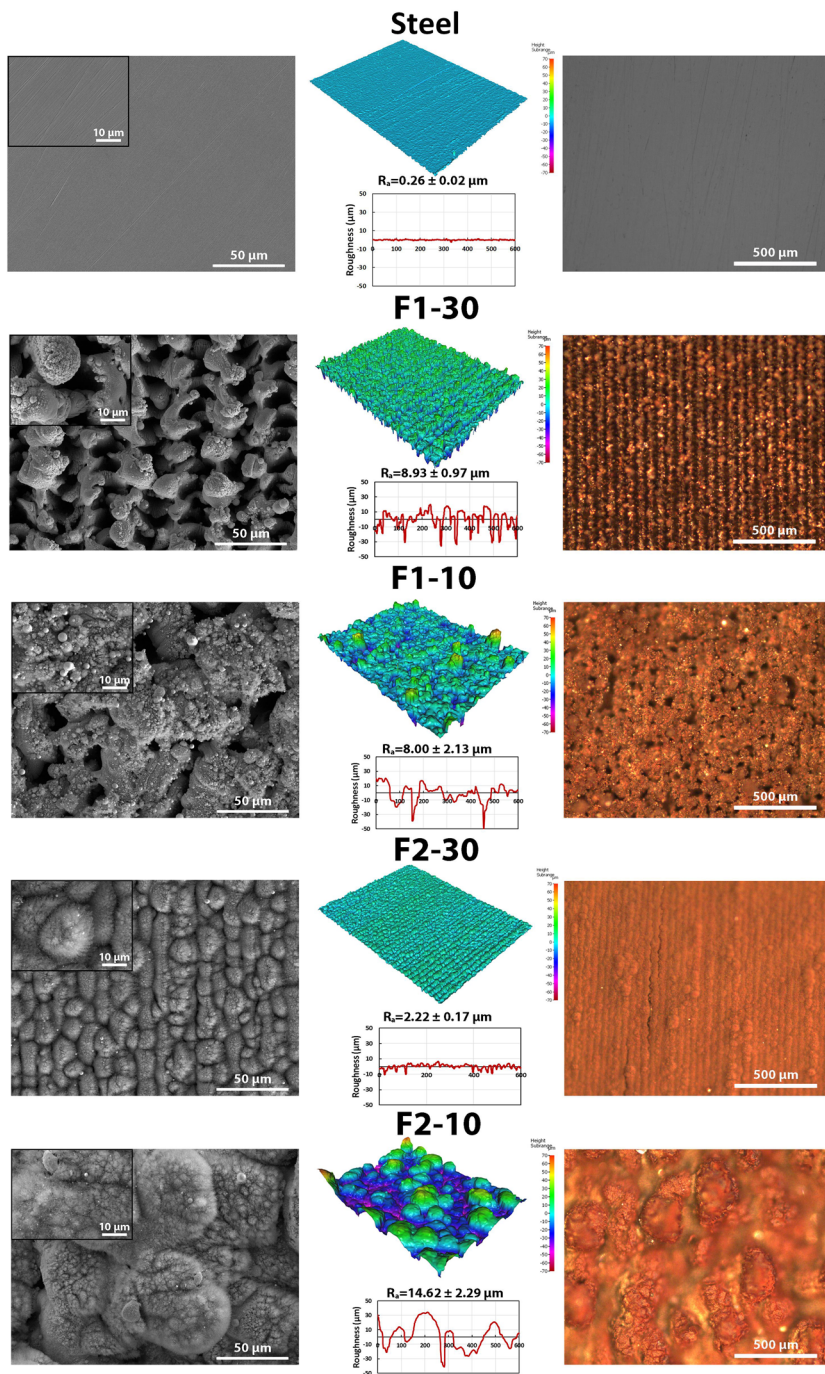
22 July 2024 17:15:15

FIG. 1. Surface topographies obtained by SEM, optical profilometry (700 × 550 μm^2), and optical microscopy for the untreated substrate and F1-30, F1-10, F2-30, and F2-10 processing conditions.

To better understand the chemical changes enacted by the different laser texturing inputs, EDX analysis of the as-received and patterned samples was performed (Table II). The concentration of oxygen, 20.0 ± 0.4 and 29.1 ± 1.6 wt. %, is larger for the conditions with the lowest scanning interval, F1-10 and F2-10, respectively. This confirms the re-melting of some areas of the stainless steel plate,

which may have been caused by the prolonged period of contact between the molten material and the open atmosphere.

Considering that the ability of bacteria to attach on surfaces is related to the capability of a droplet to interact with the surface on which it is deposited,[41] the wettability was studied through the sessile drop technique (Fig. 3). For the stainless steel plate, the
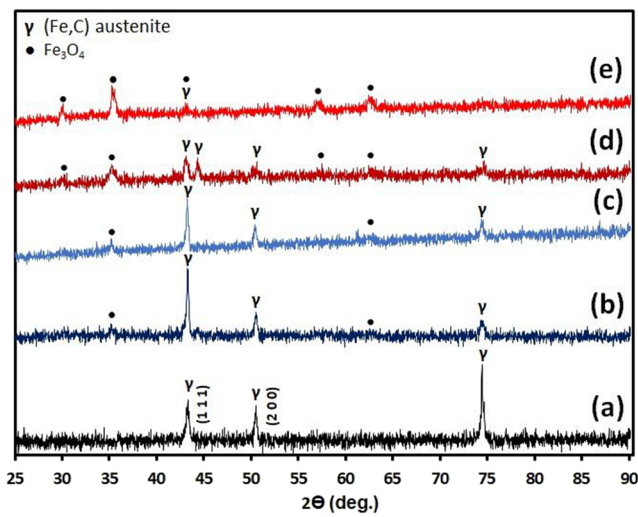
FIG. 2. XRD scans for (a) the as-received stainless steel plate and after patterning under (b) F1-30, (c) F1-10, (d) F2-30, and (e) F2-10 conditions.

contact angle measured was significantly lower (80.67° ± 3.35°) than those of the hydrophobic textured samples: 145.60° ± 3.23° (F1-30), 138.57° ± 5.02° (F1-10), 148.84° ± 1.89° (F2-30), and 143.93° ± 2.81° (F2-10). The large increase in the contact angle suggests that laser ablation has effectively modified the stainless steel surface from hydrophilic to hydrophobic (Fig. 3). Similar results are available for comparable laser textures on stainless steel surfaces, as shown by Ngo and Chun[40] and Pendurthi et al.[42] However, the reported contact angles are slightly higher than those observed in the previously mentioned studies, with values commonly in the 160°–170° region. It is also notable that a decrease in the laser scanning interval from 30 µm to 10 µm seems to lead to a reduction in the contact angle, suggesting that the less repeatable patterns are less effective in maintaining air pockets capable of sustaining the water droplet.[23]

It has been reported that the wettability of metallic textured surfaces is highly dependent on the exposure time to ambient conditions and the applied fluence. According to Kietzig et al.,[36] the texturing of stainless steel alloys, such as AISI 304L and 630 with fluences higher than 0.78 J/cm^2 results in an increase in the contact angle of about 110°–120° after 20 days at room temperature. In the present study, all measurements were performed after 3 weeks of

TABLE II. Compositional analysis (wt. %) of the stainless steel plate before and after [F1-30, F1-10, F2-30, and F2-10 laser texturing obtained through energy dispersive x-ray spectroscopy (EDX)].

	wt. %					
	O	Si	Cr	Mn	Fe	Ni
Steel	0.8 ± 0.1	0.4 ± 0.0	18.9 ± 0.1	2.0 ± 0.1	70.2 ± 0.2	7.7 ± 0.1
F1-30	17.6 ± 0.2	0.3 ± 0.0	17.7 ± 0.1	2.6 ± 0.1	56.7 ± 0.3	5.1 ± 0.1
F1-10	20.0 ± 0.4	0.4 ± 0.0	17.2 ± 0.6	2.7 ± 0.1	54.6 ± 2.1	5.1 ± 0.2
F2-30	25.8 ± 5.0	0.2 ± 0.0	15.4 ± 1.1	1.4 ± 0.1	51.5 ± 4.4	5.6 ± 0.3
F2-10	29.1 ± 1.6	0.2 ± 0.0	8.9 ± 1.2	1.3 ± 0.1	57.8 ± 2.9	2.6 ± 0.5
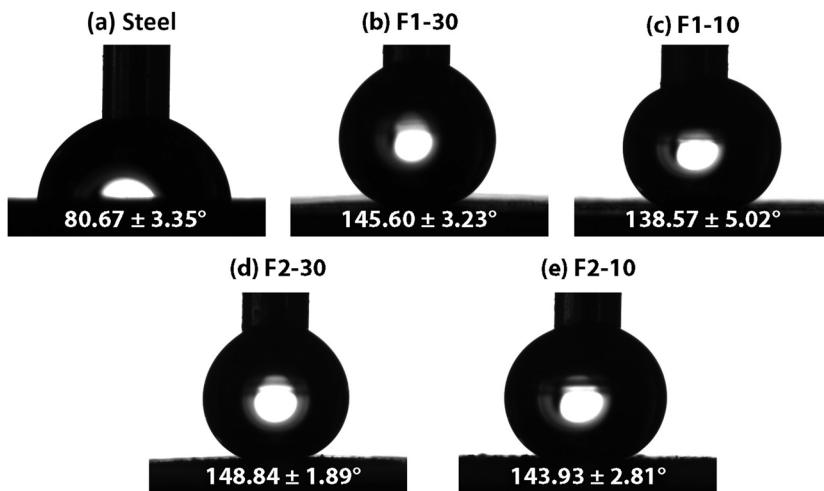
FIG. 3. Water contact angle images obtained for (a) stainless steel (control), (b) F1-30, (c) F1-10, (d) F2-30, and (e) F2-10.

laser texturing, ensuring the stability of the surface and explaining the discrepancies with Ngo and Chun's[40] and Pendurthi's[42] analyses.

The patterned surfaces present high peaks and low valleys (Fig. 1), which may be able to trap bacteria, complicating the recovering and discretization of killed bacteria that are usually straightforward in common antimicrobial tests. To account for the effect of trapped bacteria and their correlation with recovered survivors, bioluminescence measurements as well as antimicrobial tests were carried out on both as-received and textured stainless steel coupons (Fig. 4). Two images of bioluminescence after 5 min and 20 min of inoculation are shown in Fig. 4(a). The untreated stainless steel (i.e., non-oxidized) displays the highest luminescence of all samples, with a slight reduction after 20 min. As bioluminescence is released naturally by active cells and variations in luminosity depend on changes in bacterial population,[43] this increase reveals that bacteria are still growing over the contact time. This reduction is much more noticeable in the laser treated samples, indicating that physicochemical modifications enacted through laser texturing had conferred a degree of antimicrobial properties to these surfaces. Although the reduction in the light intensity occurs for all treated samples, it is, especially, evident for the F1-10 and F2-10 textures, which almost do not show any bioluminescence after 20 min of contact.

The reduction in bacteria can be appreciated in the relative intensity, I/I_{steel} (where I is the intensity of the textured sample and I_{steel} represents the intensity of the as-received stainless steel), measured during the first 20 min of contact [Fig. 4(b)]. Both F1-30 and F2-30 samples reveal an almost constant relative intensity that abruptly diminishes. For F1-30, this change takes place after 8 min followed by a reduction in the luminescence intensity of 3%/min. In contrast, a more abrupt change in the intensity (11%/min) is

observed for F2-30 after 16 min. Similarly to the F2-30 and F2-30 conditions, the F1-10 sample shows a decrease in the intensity of 3%/min, but this occurs steadily over contact time. In contrast, the bioluminescence exhibited by F2-10 does not practically change with the contact time, being the lowest of all considered conditions. These results indicate that the density of *E. coli* bacteria is reduced by the patterned samples after 30 min of contact time. Considering the interest in having surfaces with a rapid killing effect to prevent horizontal transmission from one individual to another, it is evident that the best option is laser texturing under F2-10 conditions.

Bioluminescence provides a quick assessment of the interaction between the surfaces and the bacterial species; however, quantitative analysis similar to those proposed by JIS Z2801:2010 "Antibacterial products—Test for antibacterial activity and efficacy" standard are more predominant in the field.[11] To complement the bioluminescence tests, recovery assays based on this standard were performed [Fig. 4(c) and Table III] resulting in similar results for most of the laser textures.

The quantification of colony forming units per milliliter (CFU/ml) from the untreated stainless steel is not considerably modified; however, all the textured samples display antimicrobial properties with different degrees of effectivity. The least bactericidal patterning is F2-30 with a maximum antimicrobial activity of 0.65 after 2 h and 30 min, which is in agreement with the high luminescence [Fig. 4(b)]. On the other hand, F1-30 shows the second lowest amount of recovered bacteria after 30 min of contact killing, but suddenly increases to be the highest antibacterial patterning analyzed (i.e., antimicrobial activity of 3.09). In contrast, F2-10 displays high initial antimicrobial behavior (2.28 at 30 min), which is then also maintained over the next 2 h (2.47 after 2 h 30 min),
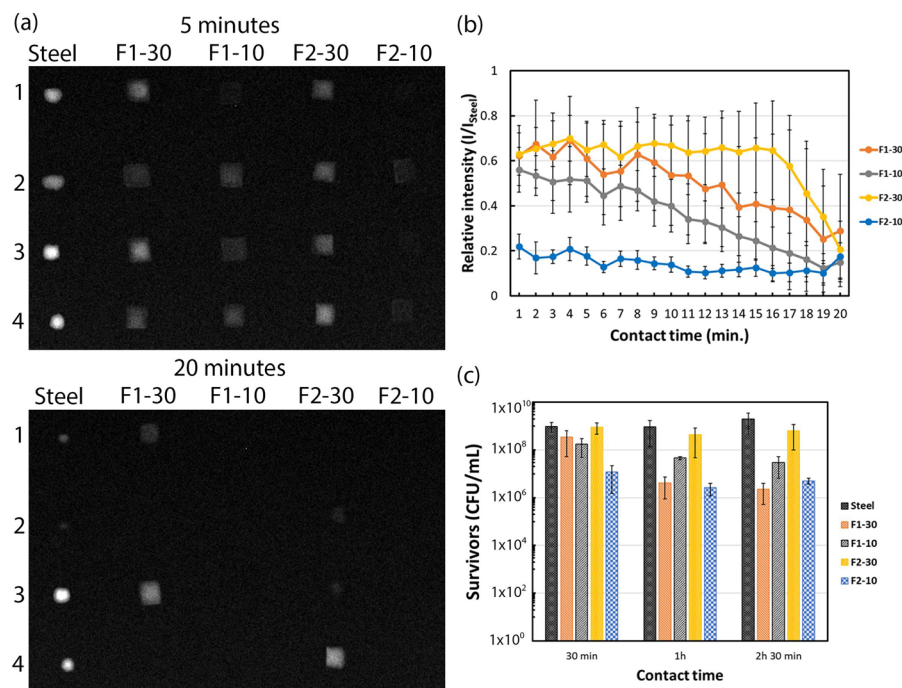
FIG. 4. Image showing the (a) bioluminescence imaging of the stainless steel samples after 5 min and 20 min of contact, (b) relative luminescence measurements of the treated samples, and (c) the number of viable bacteria recovered after 30 min, 1 h, and 2 h 30 min contact time.

TABLE III. Antimicrobial activity calculated following JIS Z2801:2010 "Antibacterial products—Test for antibacterial activity and efficacy" standard.[11]

	$\mathrm{Log_{10}}$ reduction		
	Contact time		
Sample	30 min	1 h	2 h 30 min
F1-30	0.55	2.33	3.09
F1-10	0.87	1.68	1.84
F2-30	0.04	0.33	0.65
F2-10	2.28	2.46	2.47

agreeing with the rapid reduction in bioluminescence [Fig. 4(a)]. The antimicrobial activity of sample F1-10 is similar to the trend observed in the bioluminescence tests, steady and almost constant, increasing from 0.87 up to 1.84 during the contact times studied. Nevertheless, it must be mentioned that bioluminescence assays suggest a similar antimicrobial effect in F2-30 and F2-10 after 20 min of contact killing, contrasting with the $\mathrm{log_{10}}$ reduction observed after 30 min obtained from the recovery tests. This discrepancy in the bioluminescence assay may be caused by a reduction in sensitivity for low viable CFUs as a consequence of the low bacterial inoculum used in the present assay, 2 μl and the large distance between the photomultiplier and the analyzed surface.[43] Thus, albeit promising bioluminescence tests require specific fine tuning to be comparable to standardized assays.

Biofilm formation enables bacterial species to survive in detrimental environments, requiring an increase in antibiotic concentration necessary for their eradication, which can be up to 1000 higher than planktonic cells.[44] To understand the effect of laser texturing on heavy biofilm-associated micro-organisms, we investigated the ability of a hyper-producing *A. baumannii* MAR002 strain to colonize the manufactured laser ablated stainless steel surfaces (Fig. 5). The recovery of cultured cells after 48 h revealed similar levels of bacterial growth [Fig. 5(a)] between the base substrate, 12 333 ± 5312.46 CFU/ml and F1-10, 13 893.12 ± 4687.16 CFU/ml, with a slight reduction in colony forming units for the F1-30 and F2-10, 8706.67 ± 4493.12 CFU/ml and 8683.33 ± 457.26 CFU/ml, respectively. Interestingly, the F2-30 sample showed an increase in the bacterial presence, 17 333.33 ± 3091.21 CFU/ml; nevertheless, these values are one order of magnitude lower than those obtained for common polystyrene surfaces (140 666.67 ± 14 817.41 CFU/ml).

The quantification of biomass through recovery tests does not take into account the important aspects in biofilm production, such as matrix maturity and cohesiveness. Hence, we analyzed the state of the hyper-producing bacterial strain through SEM imaging [Fig. 5(b)]. In these micrographs, the base substrate and the laser textured stainless steel further supported the low *A. baumannii* load recovered. In all cases, individualized cells with limited bacteria agglomeration were found [see arrows in inset of Fig. 5(b)] without any extracellular polymeric matrix visible, contrasting with the remarkable ability to form biofilms on the plastic surfaces (polystyrene) shown in previous studies.[35] This lack of visible aggregation followed by the production of extracellular polymeric substances suggests the ability of the textured stainless steel substrates
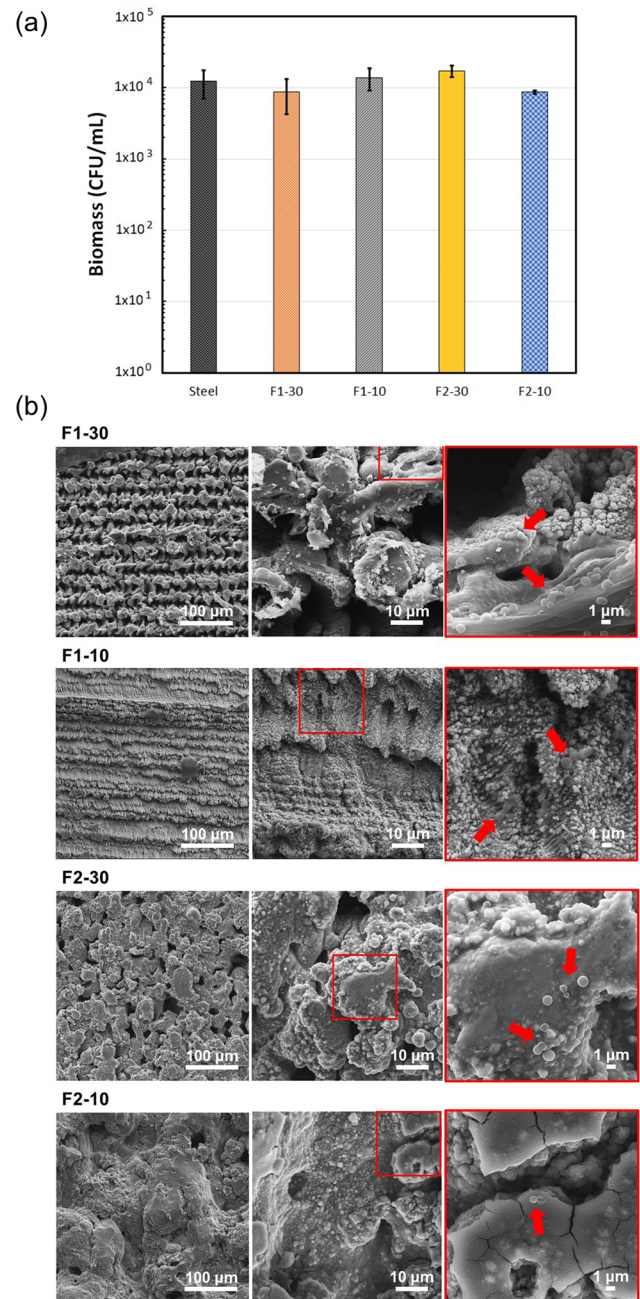
FIG. 5. *Acinetobacter baumannii* MAR002 biofilm analysis, including (a) biomass quantification and (b) SEM images of the F1-30, F1-10, F2-30, and F2-10 laser textured surfaces after 48 h.

to disrupt biofilm formation. It must be said that the reduction in the bacterial load caused by laser texturing is relatively small to that showcased against the analyzed *E. coli* species. However, similar trends are still noticeable, with the F2-10 sample being the most effective anti-adherent surface followed by F1-30.

These results show that systematically optimizing laser texturing conditions may enable the tuning of antimicrobial behavior and bacterial adhesion in stainless steel surfaces. Recent research studies have been focused on the development of superhydrophobic antifouling surfaces,[28–30] as a response to the generally accepted hypothesis that the hydrophobic materials are less prone to bacterial adhesion than hydrophilic surfaces.[24,25] Nevertheless, the present study highlights that wettability cannot be taken as a simple indicator of bacterial behavior. Contact angle analysis of the textured surfaces revealed that the F2-30 sample, $148.84°$ $\pm 1.89°$, was near superhydrophobic (CA > 150°), which should have conferred some antifouling effect against bacterial species.[26–28] Nevertheless, this sample alongside the F1-10 textured surface, $138.57°$ $\pm 5.02°$, was unable to prevent bacterial proliferation for both *E. coli* and *A. baumannii*, displaying the largest amount of viable cells in all tests considered.

Magnetite (i.e., Fe_3O_4) has been demonstrated to actively produce hydroxyl radicals in the presence of hydrogen peroxide, H_2O_2, which has been correlated with bacterial death.[45–47] H_2O_2 is fundamental to redox enzymes during bacterial metabolism,[48,49] suggesting that a possible antimicrobial mechanism could stem from reactive oxygen species (ROS) production through Fenton like reactions. On the other hand, Fang *et al.*[50] showcased the ability of magnetite nanoparticles to react with dissolved molecular oxygen in water to catalyze ROS production, contributing to the antimicrobial effect of iron oxides. Nevertheless, changes in chemistry may not completely account for the effects observed in the present study. Alongside previous reports showcasing the influence of the surface finish on bacterial attachment,[19–22,51] the obtained result further supports the limitation in predicting bacterial attachment using solely wettability, suggesting the interplay of different physicochemical properties. This is further emphasized by samples F1-30 and F2-10, similar in wettability ($145.60°$ $\pm 3.23°$ and $143.95°$ $\pm 2.81°$, respectively) but differing in average roughness, 8.93 ± 0.97 μm and 14.62 ± 1.6 μm respectively (Fig. 1), and oxygen content, 17.6 ± 0.2 wt. % and 29.1 ± 2.29 μm, respectively (XRD scans in Fig. 2). Both F1-10 and F2-30 textures revealed an ability to limit bacterial growth; nonetheless, *E. coli* reduction was time dependent with the former having superior long-term effectiveness and the latter higher short-term antimicrobial behavior. Of special interest is the limited influence in bacterial growth showcased by F2-30 and F1-10, which display the lowest surface roughness, 2.22 ± 0.17 μm and 8.00 ± 2.13 μm, respectively, and the aforementioned F1-30 and F2-10 being the most effective antimicrobial surfaces. The literature commonly shows that mismatches between the bacteria size and the surface topology can affect surface colonization with roughness higher than the bacteria analyzed, leading to a larger surface area and protection against shear forces, enhancing adhesion to the desired surface.[24,52,53] In the current study, both F1-30 and F2-10 have average roughness significantly higher than the average size, ~1 μm to 2 μm,[54,55] of both gram negative bacteria analyzed, thus offering a larger space for colonization. Nevertheless, these surfaces revealed the higher antimicrobial activity further supporting the studies of Shaikh *et al.*[21] and Taylor *et al.*,[22] indicating that smooth surfaces do not always reduce bacterial attachment, while there is not a "single size that fits all."[56,57] Surface interaction with pathogenic micro-organisms is, then, a complex phenomenon dependent on topology, chemistry, and bacterial species, and it is

clear that the optimal reduction of bacterial species has to be fine-tuned by balancing modifications to all the aforementioned parameters. Similarly to hydrophobic contact angles, there is a preference in the development of textures with a comparable length-scale roughness as the bacteria considered.[19,20] However, the textures exhibiting the largest *E. coli* reductions are those with the highest average roughness, 8.93 ± 0.93 μm and 14.62 ± 2.29 μm, for F1-30 and F2-30, respectively. This coupled with the differences displayed in bacterial growth between both gram negative bacteria analyzed further support the necessity to continue and expand our understanding of how bacterial and textured surfaces interact.

Finally, it must be said that the analysis of bacterial interactions with hard surfaces is mostly performed through the JIS Z2801:2010 standard or US EPA protocol,[11,58] which requires relatively tedious seeding, recovery, and cultivation to quantify viable cells. Bioluminescence has been recently proposed as a cost effective tool for the assessment of antimicrobial behavior in copper based materials.[43,59] The present work has shown that bioluminescence assays correlate with recovery and quantification assays in the textured stainless steel, suggesting the ability of bioluminescence to facilitate the early quantification of antimicrobial properties of hard surfaces. Nonetheless, fine-tuning is still necessary to ensure that this novel method is comparable to already standardized assays.

CONCLUSIONS

In the present work, a comprehensive analysis of the influence of laser texturing on the physicochemical and bacterial proliferation properties of stainless steel 304 has been conducted. The main findings of this study can be summarized as follows:

- Roughness measurements further supported the change in surface finish upon laser texturing revealed by electron microscopy. The average roughness of the as-received stainless steel (0.26 ± 0.02 μm) increased up to a maximum of 14.62 ± 2.29 μm for a fluence and a scanning interval of 5.64 J/cm^2 and 10 μm, respectively, with different combinations of these parameters resulting in R_a values from 2 μm to 9 μm.
- Laser treatment was observed to cause the oxidation of the stainless steel substrate in the form of Fe_3O_4, which was maximum for the 5.64 J/cm^2 treated samples.
- Sessile drop tests showed a change from hydrophilic, $80.67°$ $\pm 3.35°$, to hydrophobic with values ranging from 138° to 148°, after laser texturing. Notably, no simple correlation between the contact angle and bacterial growth was observed. The combination of roughness, chemistry, and wettability is the main driver of bacterial proliferation.
- Antimicrobial tests performed with bioluminescent *E. coli* K12 revealed a higher reduction in the bacterial load for the extreme laser conditions of the study with a maximum antimicrobial activity of 3.09 obtained after 2 h 30 min.
- Physicochemical analysis and antimicrobial analysis of *E. coli* and hyper biofilm producing *A. baumannii* MAR002 revealed that the best texturing conditions for antibacterial surface applications were achieved with a fluence of 5.64 J/cm^2, a scanning speed of 20 mm/s, and a scanning interval of 10 μm.

Overall, the present study demonstrates the ability of laser texturing to modify common engineering surfaces to confer antimicrobial properties of high interest to limit bacterial proliferation and nosocomial infections in healthcare environments.

ACKNOWLEDGMENTS

DATA AVAILABILITY

The data that support the findings of this study are available from the corresponding author upon reasonable request.

REFERENCES

[1] R. M. Klevens, J. R. Edwards, and C. L. Richards, Public Health Rep. **122**(2), 160 (2007).

[2] M. Haque, M. Sartelli, J. McKimm, and M. B. Abu Bakar, Infect. Drug Resist. **11**, 2321 (2018).

[3] National Institute of Health and Care Excellence (NICE), "Infection: Prevention and Control of Healthcare Associated Infections in Primary and Community Care, Clinical Guideline CG139" (NICE, UK, 2017).

[4] S. B. Levy, *The Antibiotic Paradox: How Miracle Drugs are Destroying the Miracle* (Springer, 2013).

[5] D. Jasovský, J. Littmann, A. Zorzet, and O. Cars, Upsala J. Med. Sci. **121**(3), 159 (2016).

[6] A.-P. Magiorakos, A. Srinivasan, R. B. Carey, Y. Carmeli, M. E. Falagas, C. G. Giske, S. Harbarth, J. F. Hindler, G. Kahlmeter, B. Olsson-Liljequist, D. L. Paterson, L. B. Rice, J. Stelling, M. J. Struelens, A. Vatopoulos, J. T. Weber, and D. L. Monnet, Clin. Microbiol. Infect. **18**(3), 268 (2012).

[7] J. O'Neill, S. Davies, J. Rex, L. J. White, and R. Murray, "Review on antimicrobial resistance, tackling drug-resistant infections globally: Final report and recommendations" (Wellcome Trust and UK Government, London, 2016).

[8] M. E. de Kraker, A. J. Stewardson, and S. Harbarth, PLoS Med. **13**(11), e1002184 (2016).

[9] A. Różańska, A. Chmielarczyk, D. Romaniszyn, M. Bulanda, M. Walkowicz, P. Osuch, and T. Knych, Antimicrob. Resist. Infect. Control **6**(1), 80 (2017).

[10] S. J. Dancer, L. F. White, J. Lamb, E. K. Girvan, and C. Robertson, BMC Med. **7**(1), 28 (2009).

[11] V. Villapún, L. Dover, A. Cross, and S. González, Materials **9**, 736 (2016).

[12] C. E. Santo, E. W. Lam, C. G. Elowsky, D. Quaranta, D. W. Domaille, C. J. Chang, and G. Grass, Appl. Environ. Microbiol. **77**, 794 (2011).

[13] S. L. Warnes and C. W. Keevil, PLoS One **8**, e75017 (2013).

[14] T. Mori, T. Kikuchi, M. Sakurai, J. Kato, Y. Koda, R. Abe, C. Sumiya, R. Yamazaki, K. Sugita, N. Hasegawa, and S. Okamoto, Rinsho Ketsueki **60**(1), 3 (2019).

[15] B. de Jong, A. M. Meeder, K. W. A. C. Koekkoek, M. A. Schouten, P. Westers, and A. R. H. van Zanten, J. Hosp. Infect. **99**(3), 256 (2018).

[16] L. C. Hsu, J. Fang, D. A. Borca-Tasciuc, R. W. Worobo, and C. I. Moraru, Appl. Environ. Microbiol. **79**, 2703 (2013).

[17] K. A. Whitehead, J. Colligon, and J. Verran, Colloids Surf., B **41**, 129 (2005).

[18] R. S. Friedlander, H. Vlamakis, P. Kim, M. Khan, R. Kolter, and J. Aizenberg, Proc. Natl. Acad. Sci. U. S. A. **110**, 5624 (2013).

[19] I. Carvalho, M. Henriques, and S. Carvalho, *Microbial Pathogens and Strategies for Combating Them: Science, Technology and Education* (Formatex Research Center, 2013).

[20] M. Á. Pacha-Olivenza, R. Tejero, M. C. Fernández-Calderón, E. Anitua, M. Troya, and M. L. González-Martín, BioMed Res. Int. **2019**, 1 (2019).

[21] S. Shaikh, D. Singh, M. Subramanian, S. Kedia, A. K. Singh, K. Singh, N. Gupta, and S. Sinha, J. Non-Cryst. Solids **482**, 63 (2018).

[22] R. L. Taylor, J. Verran, G. C. Lees, and A. J. P. Ward, J. Mater. Sci.: Mater. Med. **9**, 17 (1998).

[23] K. J. Kubiak, M. C. T. Wilson, T. G. Mathia, and P. Carval, Wear **271**, 523 (2011).

[24] F. Song, H. Koo, and D. Ren, J. Dent. Res. **94**, 1027 (2015).

[25] T. Wassmann, S. Kreis, M. Behr, and R. Buergers, Int. J. Implant. Dent. **3**, 32 (2017).

[26] J. Li, G. Wang, Q. Meng, C. Ding, H. Jiang, and Y. Fang, Appl. Surf. Sci. **315**, 407 (2014).

[27] X. Pu, G. Li, and H. Huang, Biol. Open **5**(4), 389 (2016).

[28] C. Sciancalepore, L. Gemini, L. Romoli, and F. Bondioli, Surf. Coat. Technol. **352**, 370 (2018).

[29] Q. Ma, Z. Tong, W. Wang, and G. Dong, Appl. Surf. Sci. **455**, 748 (2018).

[30] D.-M. Chun, C.-V. Ngo, and K.-M. Lee, CIRP Ann. **65**(1), 519 (2016).

[31] S. Li, Y. Liu, Z. Zheng, X. Liu, H. Huang, Z. Han, and L. Ren, Chem. Eng. J. **372**, 852 (2019).

[32] K. Sun, H. Yang, W. Xue, A. He, D. Zhu, W. Liu, K. Adeyemi, and Y. Cao, Appl. Surf. Sci. **436**, 263 (2018).

[33] A. H. A. Lutey, L. Gemini, L. Romoli, G. Lazzini, F. fuso, M. Faucon, and R. Klin, Sci. Rep. **8**, 10112 (2018).

[34] World Health Organization, "Prioritization of pathogens to guide discovery, research and development of new antibiotics for drug resistant bacterial infections, including tuberculosis," WHO/EMP/IAU/2017.12 (WHO, Geneva, 2017).

[35] L. Álvarez-Fraga, A. Pérez, S. Rumbo-Feal, M. Merino, J. A. Vallejo, E. J. Ohneck, R. E. Edelmann, A. Beceiro, J. C. Vázquez-Ucha, J. Valle, L. A. Actis, G. Bou, and M. Poza, Virulence **7**(4), 443 (2016).

[36] A. M. Kietzig, S. G. Hatzikiriakos, and P. Englezos, Langmuir **25**(8), 4821 (2019).

[37] S. Moradi, S. G. Hatzikiriakos, and S. Kamal, Surf. Innovations **3**, 1 (2015).

[38] B. Wu, M. Zhou, J. Li, X. Ye, G. Li, and L. Cai, Appl. Surf. Sci. **256**(1), 61 (2009).

[39] International Centre for Diffraction Data, Diffraction Standard, PDF: 00-031-0619, 2014 [Joint Committee on Powder Diffraction Standards (JCPDS), 2014].

[40] C.-V. Ngo and D.-M. Chun, Appl. Surf. Sci. **409**, 232 (2017).

[41] L. K. Ista, S. Mendez, and G. P. Lopez, Biofoulding **26**, 111 (2010).

[42] A. Pendurthi, S. Movafaghi, W. Wang, S. Shadman, A. P. Yalin, and A. K. Kota, ACS Appl. Mater. Interfaces **9**(31), 25656 (2017).

[43] M. Rosenberg, H. Vija, A. Kahru, C. W. Keevil, and A. Ivask, Sci. Rep. **8**(1), 8172 (2018).

[44] D. Sharma, L. Misba, and A. U. Khan, Antimicrob. Resist. Infect. Control **8**(1), 76 (2019).

[45] H. Wu, J.-J. Yin, W. G. Wamer, M. Zeng, and Y. M. Lo, J. Food Drug Anal. **22**(1), 86 (2014).

[46] R. Zalma, L. Bonneau, J. Guignard, H. Pezerat, and M. C. Jaurand, Toxicol. Environ. Chem. **13**(3-4), 171 (1987).

[47] M. Dryden, Int. J. Antimicrob. Agents **51**(3), 299 (2018).

[48] J. Yeom, J. A. Imlay, and W. Park, J. Biol. Chem. **285**(29), 22689 (2010).

[49] A. I. James, J. Mol. Biol. **75**(6), 1389 (2010).

[50] G.-D. Fang, D.-M. Zhou, and D. D. Dionysiou, J. Hazard. Mater. **250-251**, 68 (2013).

[51] S. C. Cox, P. Jamshidi, N. M. Eisenstein, M. A. Webber, H. Burton, R. J. A. Moakes, O. Addison, M. Attallah, D. E. T. Shepherd, and L. M. Grover, ACS Biomater. Sci. Eng. **3**(8), 1616 (2017).

[52] S. Achinas, N. Charalampogiannis, and G. J. W. Euverink, Appl. Sci. **9**(14), 2801 (2019).

[53] R. J. Crawford, H. K. Webb, V. K. Truong, J. Hasan, and E. P. Ivanova, Adv. Colloid Interface Sci. **179-182**, 142 (2012).

[54] S. S. Board and National Research Council, *Size Limits of Very Small Microorganisms: Proceedings of a Workshop* (National Academies Press, USA, 1999).

[55] S. B. Almasaudi, Saudi J. Biol. Sci. **25**(3), 586 (2018).

[56] F. Riedewald, PDA J. Pharm. Sci. Technol. **60**(3), 164 (2016).

[57] L. D. Renner and D. B. Weibel, MRS Bull. **36**, 347 (2011).

[58] L. B. Boinovich, V. V. Kaminsky, A. G. Domantovsky, K. A. Emelyanenko, A. V. Aleshkin, E. R. Zulkarneev, and A. M. Emelyanenko, Langmuir **35**(7), 2832 (2019).

[59] V. M. Villapún, B. Qu, P. A. Lund, W. Wei, L. G. Dover, J. R. Thompson, J. O. Adesina, C. Hoerdemann, S. Cox, and S. González, Mater. Today Commun. **23**, 101074 (2020).

22 July 2024 17:15:15